

Electromagnetic Spectrum from QGP Fluid ^{*}

Tetsufumi Hirano^{1 †}, Shin Muroya^{2 ‡}, and Mikio Namiki^{1 §}

¹*Department of Physics, Waseda University
Tokyo 169, Japan*

²*Tokuyama Women's College
Tokuyama, Yamaguchi 754, Japan*

(November 19, 2018)

Abstract

We calculate thermal photon and electron pair distribution from hot QCD matter produced in high energy heavy-ion collisions, based on a hydrodynamical model which is so tuned as to reproduce the recent experimental data at CERN SPS, and compare these electromagnetic spectra with experimental data given by CERN WA80 and CERES. We investigate mainly the effects of the off-shell properties of the source particles on the electromagnetic spectra.

^{*}A talk given at the International School on the Physics of Quark Gluon Plasma, June 3-6, 1997, Hiroshima, Japan. To be appeared in Prog. Theor. Phys. Supplement.

[†]Electronic address : 69715212@mn.waseda.ac.jp

[‡]Electronic address : muroya@yukawa.kyoto-u.ac.jp

[§]Electronic address : namiki@mn.waseda.ac.jp

I. INTRODUCTION

In high-energy heavy-ion collisions, so many kinds of secondary particles, such as hadrons, leptons and photons, come out of hot matter which is produced at an early stage of the nuclear reaction. At first, we naively expect that the particle distribution directly reflects informations concerning the hot matter. As for hadrons, however, we regret to say that the final distribution is far from the initial form of hot matter and it is dirty due to strong interaction. While photons and leptons are considered to keep the information about the hot matter, because they interact only electro-magnetically.

We analyze the thermal photon and electron pair emission from the hot matter in a consistent manner, as follows: first we choose initial parameters in our hydrodynamical model so as to fit the experimental data of hadrons. Next, we derive the thermal production rates of photon and dilepton based on a quantum Langevin equation. Finally, accumulating the production rate over the whole space-time volume, which is given by our hydrodynamical model, we obtain the electromagnetic spectra which are to be compared with experimental data.

II. RELATIVISTIC HYDRODYNAMICAL MODEL AND HADRON SPECTRUM

We first analyze recent hadron spectra at CERN SPS energy. In a previous paper [2], we solved numerically the (3+1)-dimensional hydrodynamical equation. In this paper we adopt the Bag model for the equation of state instead of the simple phase transition model discussed in Ref. [2]. Here we suppose that the fluid in the QGP phase is composed dominantly of u -, d -, s -quarks and gluons and that the fluid in the hadron phase is composed dominantly of pions and kaons. We fix the critical temperature as $T_c = 160$ MeV and the freeze-out temperature as $T_f = 140$ MeV.

Putting the initial temperature as $T_i = 209$ MeV, we can see that our hydrodynamical model well reproduce the experimental data of the pseudo-rapidity distribution of charged hadron and the transverse momentum distribution of neutral pions in the S+Au 200A GeV collisions [4]. In the case of the Pb+Pb 158A GeV collisions, the best value to reproduce the recent experimental data of the rapidity distribution of negative charged hadron and the transverse momentum distribution of neutral pions is $T_i = 190$ MeV [4].

III. THERMAL PRODUCTION RATE

As for the thermal photon and electron pair emission processes from hot matter, we can easily write general formulas of production rates for these processes [7]

$$R_\gamma = \int \frac{d^3\mathbf{k}}{(2\pi)^3 2k} \sum_\lambda \varepsilon_\mu^{(\lambda)} \varepsilon_\nu^{(\lambda)} H_{\mu\nu}(k), \quad (1)$$

$$R_{e^-e^+} = \int \frac{d^3\mathbf{p}_{e^-}}{(2\pi)^3 2\varepsilon_{e^-}} \frac{d^3\mathbf{p}_{e^+}}{(2\pi)^3 2\varepsilon_{e^+}} \times e^2 \text{Tr}[\gamma^\mu (\not{p}_{e^-} - m_e) \gamma^\nu (\not{p}_{e^+} + m_e)] \frac{1}{P^4} H_{\mu\nu}(P). \quad (2)$$

Here $H_{\mu\nu}$ is a hadronic structure tensor, which is the Fourier transform of current correlation function. Supposing that a local equilibrium system is dominated by a certain mode and that the canonical operator of the mode obeys a quantum Langevin equation [1], we replace the correlation function with the ensemble average in the sense of the quantum Langevin equation. Then we easily obtain the thermal photon production rate [3].

We can also obtain the thermal dilepton production rate based on the quantum Langevin equation in the same manner. We first consider the process of $\pi^+\pi^- \rightarrow e^-e^+$. The production rate of this process at $T = 160$ MeV is shown in Fig. 1. It is well known that this elementary process has the threshold at $M = 2m_\pi$, which is originated from the on-shell condition of the source particle. In our formalism the source particle has off-shell properties, hence, we can observe in Fig. 1 that there is no threshold effect. Assuming the Vector Meson Dominance, we multiply the production rate by the square of pion electromagnetic form factor. In Fig. 1, the deviation between the usual on-shell model and the off-shell model appears around the threshold and the difference is very small in the invariant mass region which is much larger than the threshold. On the other hand, because of the small value of threshold, we can safely neglect the off-shell effect in the process of $q\bar{q} \rightarrow e^-e^+$.

In the mixed phase region, We define the production rate as a function of T and λ

$$\frac{dN}{dx^4} = R(T, \lambda) = \lambda R_{\text{QGP}} + (1 - \lambda) R_{\text{had}}, \quad (3)$$

where λ is the fraction of QGP phase region. Integrating this production rate over the whole space-time volume in which the particle source exists, we obtain the momentum distribution of photon and the invariant mass distribution of electron pair which are to be compared with experimental data.

IV. RESULTS

Using together with the numerical results of our hydrodynamical model and the thermal production rate, we can predict the electromagnetic spectra. Figure 2 shows the numerical result of thermal photon distribution in S+Au 200A GeV collisions in comparison with the CERN WA80 data [5]. We can see in this figure that our model is consistent with these experimental data. We can predict the thermal photon distribution for the Pb+Pb 158A GeV collisions (Fig. 3). In Fig. 3, the photon distribution for the Pb+Pb collisions is similar to the result of the S+Au collisions. The larger space-time volume in the Pb+Pb collisions is compensated by the lower initial temperature in comparison with the S+Au experiment.

Figure 4 shows the numerical results of electron pair distribution in comparison with the experimental data given by CERN CERES [6]. The solid curve stands for the electron pair distribution of our model with $c = 1.0$ in the damping function and the dashed curve stands for the result obtained by making use of the production rate based on the perturbative method neglecting off-shell property of the source current. The parameter c in the damping function has already been fixed by the previous analyses of the thermal photon production [3].

Our model based on the quantum Langevin equation was expected to enable us to reproduce the enhancement of the experimental data near the threshold $M \sim 2m_\pi$ because of the off-shell properties of the source current (see also Fig. 1). However, we must say

from Fig. 4 that the off-shell property of the source particles is not enough to reproduce the enhancement in the small invariant mass region of the experimental data [8]. In this paper, we do not take account of the possibility of the partial restoration of chiral symmetry. Therefore, our results may be improved by taking into account the mass shift of ρ meson due to finite temperature effects.

V. SUMMARY

We compared our numerical results of electromagnetic spectrum with experimental data at CERN SPS energy. In the photon case our result is almost consistent with WA80 S+Au data. Furthermore, we evaluated the expected thermal photon distribution for the Pb+Pb collisions. We observed that this distribution is similar to the result of the S+Au collisions. In the case of the low mass region of electron pair distribution, our result was not improved by the off-shell property enough to explain the experimental data obtained by CERN CERES.

Acknowledgments

The authors are much indebted to Prof. I. Ohba and Prof. H. Nakazato for their helpful comments. They also thank Dr. H. Nakamura, Dr. C. Nonaka and other members of high energy physics group of Waseda Univ. for their fruitful discussions.

REFERENCES

- [1] M. Mizutani, S. Muroya and M. Namiki, Phys. Rev. **D37**, 3033 (1988).
- [2] Y. Akase, M. Mizutani, S. Muroya and M. Yasuda, Prog. Theor. Phys. **85**, 305 (1991).
- [3] T. Hirano, S. Muroya and M. Namiki, Prog. Theor. Phys. **98**, 129 (1997).
- [4] C. Nonaka, talk at *International Workshop on Physics of Relativistic Heavy Ion Collisions, YITP, Kyoto, Japan, 1997* (unpublished); S. Muroya and C. Nonaka, in preparation.
- [5] R. Albrecht et al. : WA80, Phys. Rev. Lett. **76**, 3506 (1996).
- [6] G. Agakichiev et al. : CERES Collaboration, Phys. Rev. Lett. **75**, 1272 (1995).
- [7] L. D. McLerran and T. Toimera, Phys. Rev. **D31**, 545 (1985).
- [8] It is noted that Sollfrank et al. obtained similar result by making use of their hydrodynamical model: J. Sollfrank, P. Huovinen, M. Kataja, P. V. Ruuskanen, M. Prakash and R. Venugopalan, Phys. Rev. **C55**, 392 (1997).

FIGURE CAPTION

FIG. 1 The production rate of the process $\pi^+\pi^- \rightarrow e^-e^+$. The curve $c = 0$ is the same result as the perturbation theory.

FIG. 2 Thermal photon distribution in the S+Au 200A GeV collisions. The solid curve stands for the photon distribution of our numerical result.

FIG. 3 Expected thermal photon distribution. The solid curve stands for the expected thermal photon spectrum in the Pb+Pb 158A GeV collisions. We also represent the result of S+Au collisions for comparison.

FIG. 4 Electron pair invariant mass distribution.

Production Rate

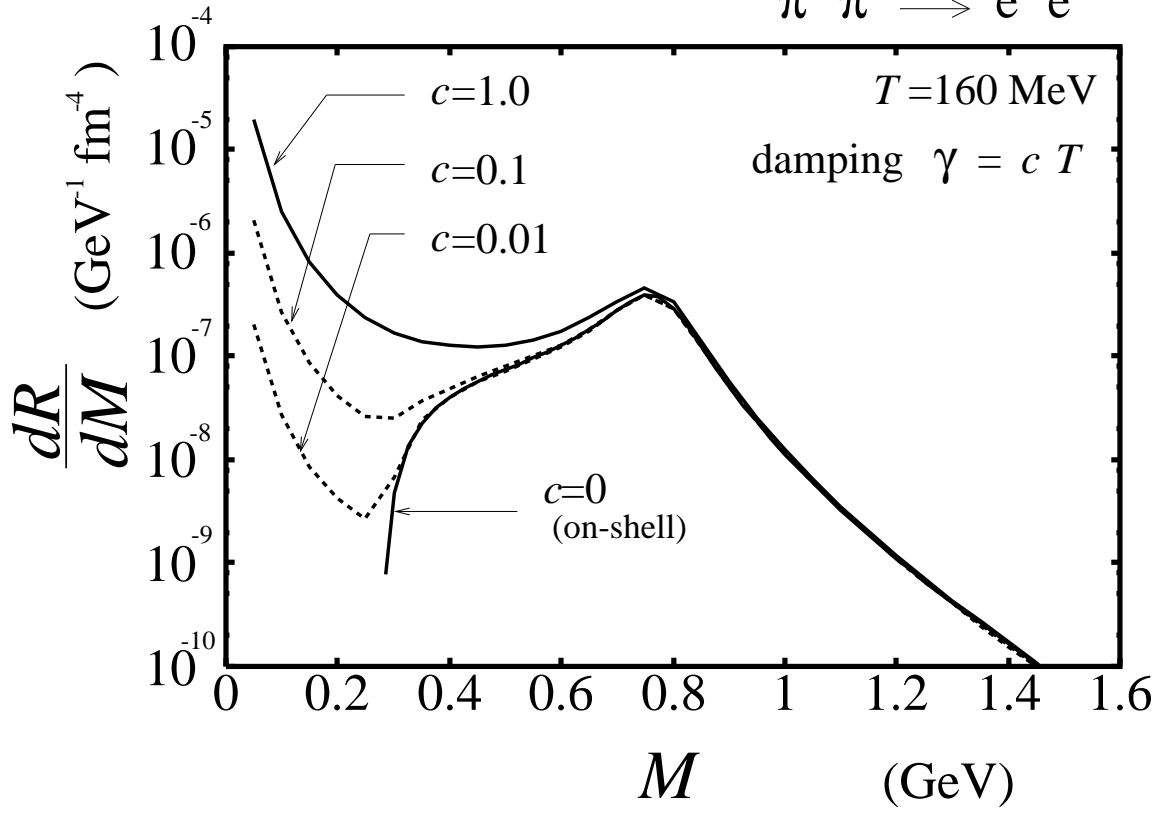
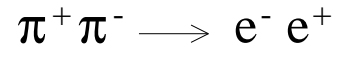


Fig. 1

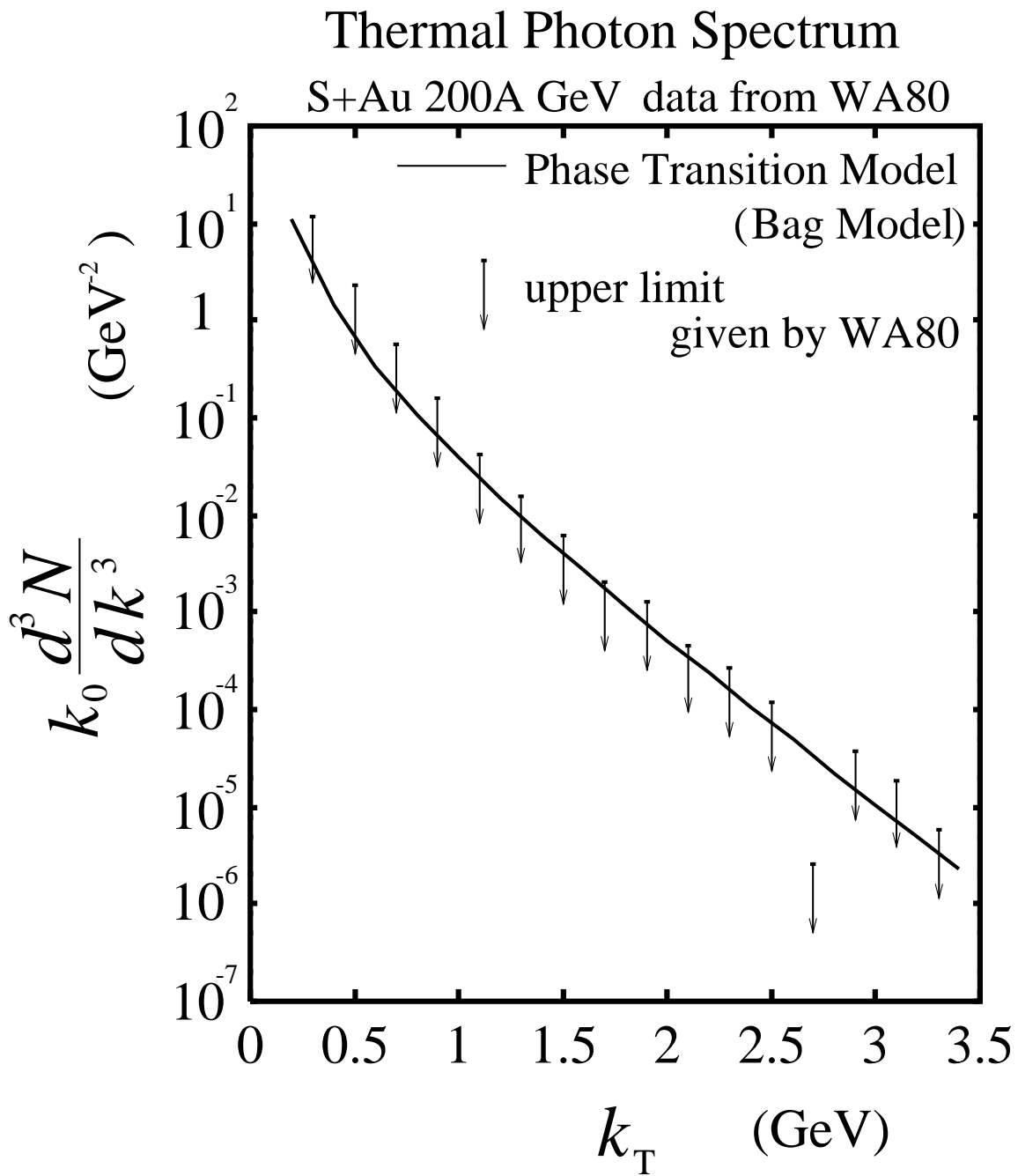


Fig. 2

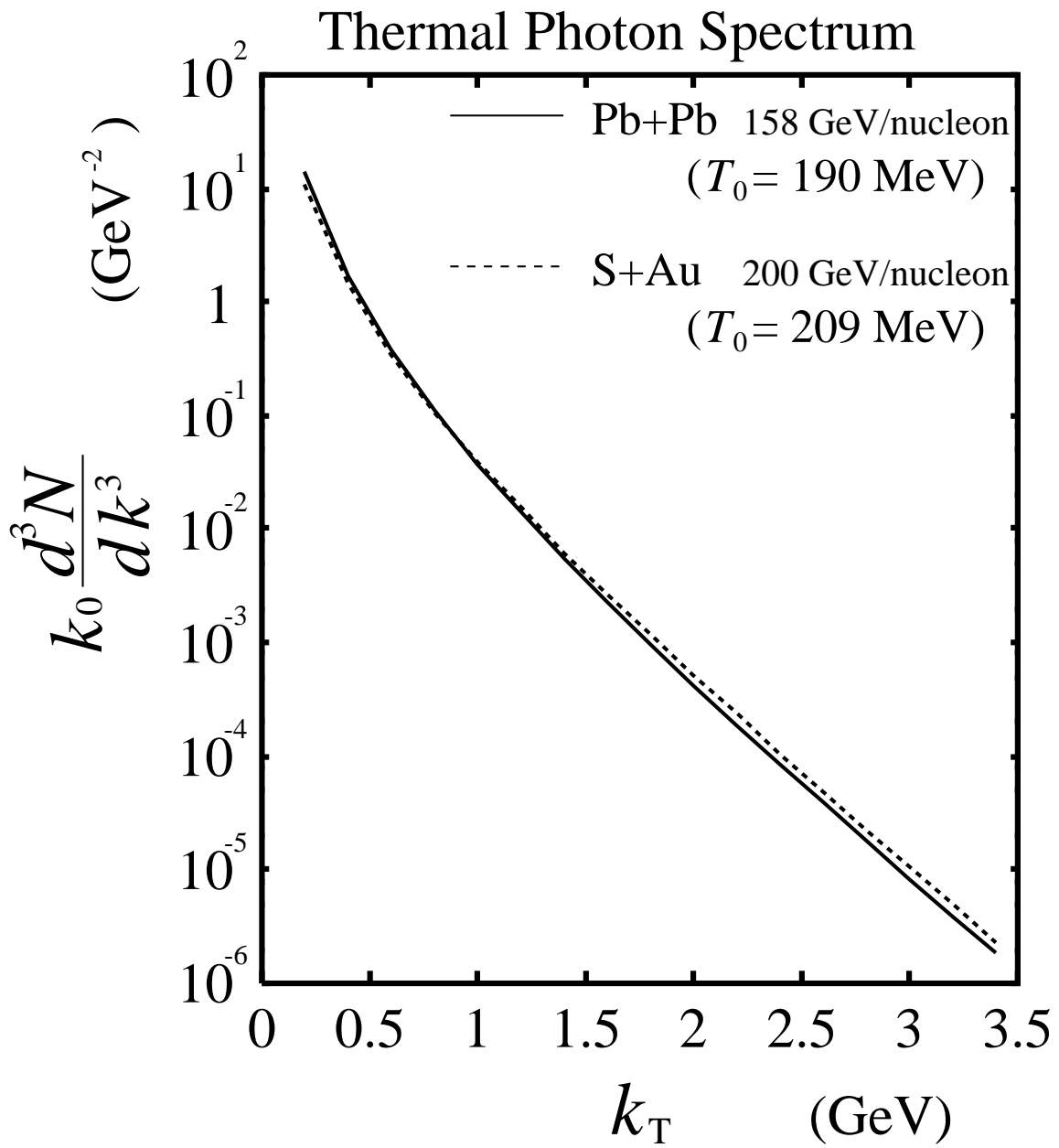


Fig. 3

Electron Pair Invariant Mass Distribution

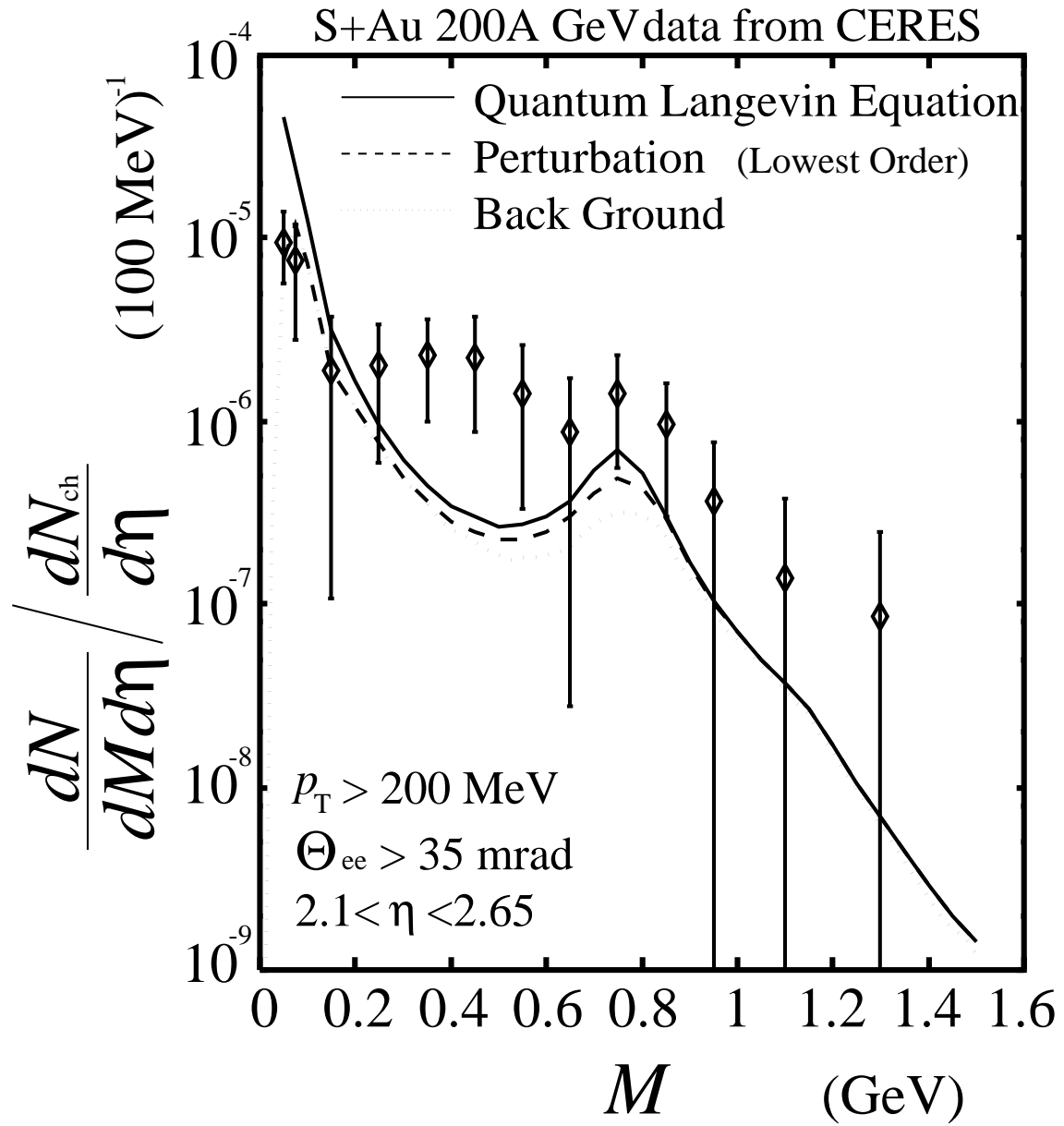


Fig. 4